A GEOCHEMICAL MODEL OF THE KILAUEA EAST RIFT ZONE

By Donald Thomas

ABSTRACT

The east rift zone of Kilauea Volcano is comprised of a northeast- to southwest-trending complex of dikes and fractures extending more than 100 kilometers from the summit caldera to the ocean floor. Geologic, petrologic, and geophysical data indicate that substantial volumes of molten magma are intruded into and stored within the east rift dike complex and that parts of the rift have temperatures exceeding the Curie point of basalt. The shallow ground-water hydrology and chemistry on the lower rift are strongly affected by natural thermal discharge from the rift and indicate a continuous heat loss rate estimated at 291 megawatts of thermal energy. Several deep geothermal wells drilled into the lower rift have confirmed the presence of high temperatures and of an active hydrothermal system associated with the rift. The maximum temperatures encountered in the deep wells approach the critical point of water (374 °C) but show a sharp decline on the southern boundary of the rift. Petrologic studies of drill cuttings from the deep geothermal wells have shown that intermittent, intense hydrothermal alteration has occurred to depths of at least 2.5 km. The alteration phases present indicate that metamorphism reaches the greenschist facies and have strong similarities to alteration suites found in midocean-ridge hydrothermal systems. Chemical data from the deep fluids suggest that the primary source of recharge to the reservoir is meteoric water in the interior of the rift but that saline water is present on the southern boundary. Production data from the deep wells also indicate that accessible parts of the hydrothermal system are capable of producing both dry steam and hot brine. The data that have been gathered to the present indicate that the hydrothermal system associated with the Kilauea east rift zone is actively evolving and has characteristics ranging from low-temperature benign fluids to high-temperature, highly aggressive fluids that may provide both an economically viable geothermal resource and a natural laboratory for the study of ore-forming and geochemical-cycling processes.

INTRODUCTION

Exploration for geothermal resources in Hawaii began in 1962 when four shallow wells were drilled into the Kilauea lower east rift zone (LERZ) (fig. 56.1; table 56.1) in an effort to develop a commercial steam resource. Although all four wells encountered above-ambient temperatures, none discovered an economically useful steam or hot-water resource. A second effort to study the deep thermal conditions on the Kilauea east rift zone (ERZ) was initiated in 1972 under funding from the National Science Foundation. This effort culminated in the drilling and completion of the 1,966-meter-deep Hawaii Geothermal Project well A (HGP-A) in 1976. Testing of this well indicated that temperatures of 358 °C were present at the bottom of the hole and that the well was capable of producing approximately 48 tonnes per hour (t/h) of steam and hot water. A geothermal generator facility was installed on this well in 1981 and, as of July 1985, has been in operation for approximately 44 months. Subsequent to the completion and initial testing of HGP-A, six privately financed deep exploration wells have been drilled into the LERZ. The data that have been obtained from the deep exploratory drilling into the rift and from the long-term discharge of HGP-A have now provided us with sufficient information to develop a preliminary model of the hydrothermal system associated with the ERZ.

ACKNOWLEDGMENTS

The research results reported here have been made possible only through the capable assistance and willing cooperation of numerous very able individuals. Field and laboratory assistance by M. Dahlstrom, C. Fraley, D. Mills, J. McCullough, B. Taylor, L. Bergknut, E. DeCarlo, K.E. Cuff, M.E. Cox, R. Mitiguy, and R. Kochy is gratefully acknowledged. The cooperation and assistance of the Hawaii Geothermal Project staff—J. Shupe, P. Yuen, and L. Lopez—and Hawaii Electric Light Company—N. Oss, F. Kennedy, N. Uchida, and G. Jenkins—have been instrumental in allowing this research to be conducted. Thanks also are due to C. Zablocki, D. Jackson, R. Moore, A. Truesdell, and C.E. Helsley for helpful discussion during the evolution of this model. A special notice of appreciation is also due to Barnwell Geothermal Corporation and Geothermex Inc. for allowing access to their data and providing samples from their wells.

Funding for this work has come principally from the U.S. Department of Energy and the State of Hawaii Department of Planning and Economic Development with additional funding from Hawaiian Electric Industries and the Electric Power Research Institute.

The assistance of L. Kajiwara in drafting and of C. Koyanagi in manuscript preparation is gratefully acknowledged.

Hawaii Institute of Geophysics Contribution No. 1702.

GEOLOGIC SETTING

The east rift zone, a major structural feature of Kilauea Volcano, extends from the summit caldera in an easterly direction for approximately 50 km, where it enters the ocean and continues as a

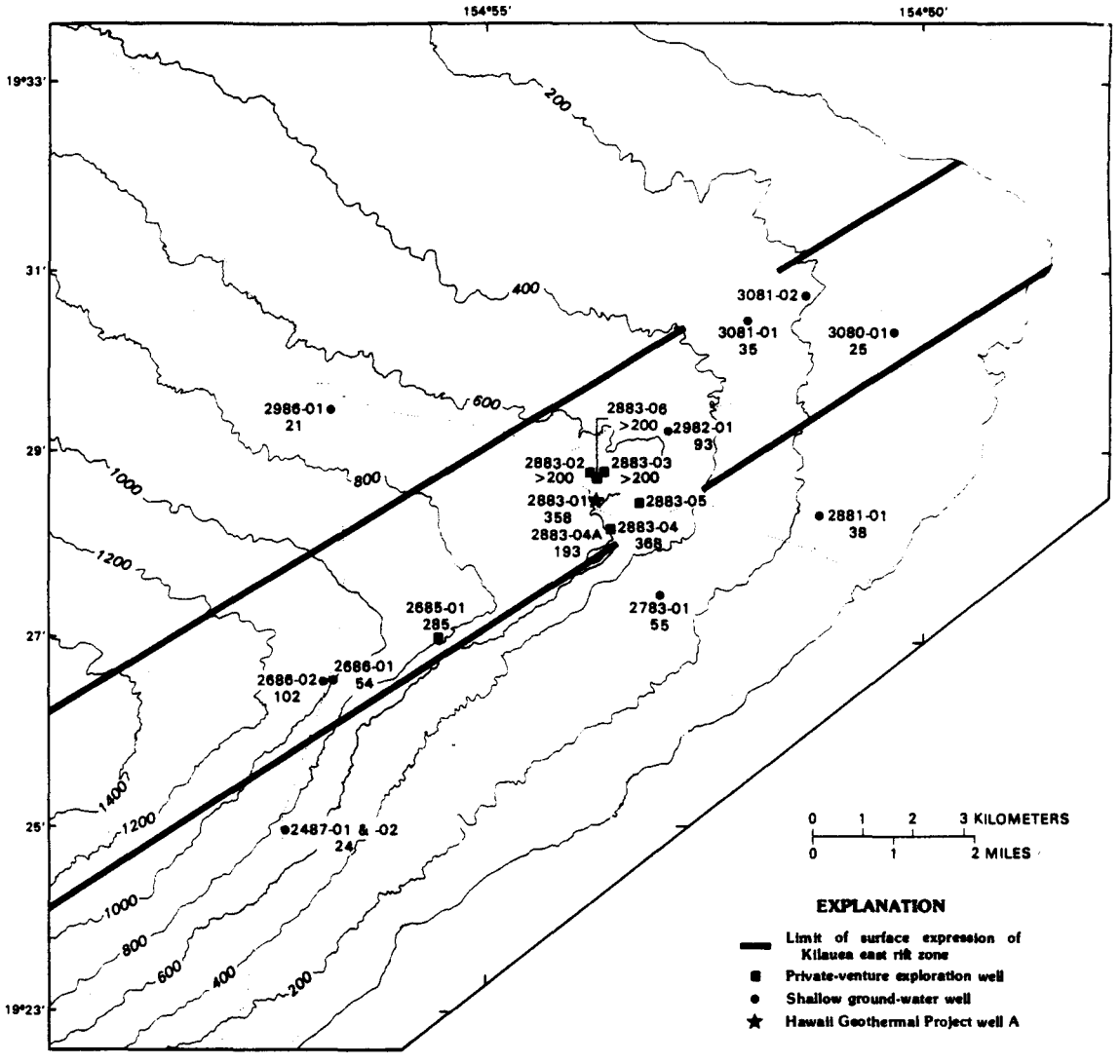

FIGURE 56.1.—Kilauea lower east rift zone showing locations of ground-water and geothermal exploration wells. Well-identification numbers and temperature (in degrees Celsius), if known, are given next to symbols. Dashed lines represent roads.

submarine ridge for another 50–60 km. Geologic mapping on Kilauea and studies of eroded rift systems on the older islands of the Hawaiian Chain indicate that the structure of the rift is composed of hundreds to thousands of near-vertical thin tabular dikes interspersed with highly fractured country rock (Macdonald and Abbott, 1970). The trend of the individual dikes parallels the strike of the rift, and the dip angles of both the fractures and dikes typically deviate by only a few degrees from vertical (Macdonald and Abbott, 1970).

The mechanism responsible for the formation of the ERZ is believed to be the forceful intrusion of magma from the summit magma reservoir into the rift system at depths of 3–6 km beneath the summit (Fiske and Jackson, 1972). The occurrence of these intrusive events, typically indicated by seismic and deformation changes both at the summit and in the area of an intrusion, may result in a surface eruption or in the formation of a subsurface dike. Although the rate of magma intrusion in the rift zone is not well known, theoretical studies have inferred deposition rates as high as

TABLE 56.1.—*Characteristics of geothermal exploration wells drilled on the Kilauea east rift zone*

Well	Name	Depth (meters)	Bottom temperature (°C)	Comments
2685-01	Ashida-1	2,530	326	Insufficient permeability to sustain production; suspended.
2686-01	Geothermal-1	54.3	54	Drilled 1962, did not reach water table; abandoned.
2686-02	Geothermal-2	169.5	102	Drilled in 1962, did not reach water table; abandoned.
2883-01	HGP-A	1,967	358	Sustained production of 50 t/h of brine and steam.
2883-02	Kapoho State 1	2,222	339	Production rate of 32.7 t/h was achieved during short test; operation suspended.
2883-03	Kapoho State 2	2,440	342	Production rate of 15 t/h was achieved during short test; operation suspended.
2883-04	Lanipuna-1	2,557	>363	High salinity at intermediate depth and temperature, low permeability at depth; abandoned.
2883-04A	Lanipuna-1	1,920	149	Drilled as a slant hole off of 2983-02, maximum temperature of 193 °C with temperature turnover; abandoned.
2883-05	Lanipuna-6			Very productive low-temperature aquifer encountered at 1,370-m depth.
2883-06	Kapoho State 1A	2,000	300	Drilled in 1984; short-duration testing produced self-sustaining flow; production rate and subsurface temperature data are presently proprietary.
2982-01	Geothermal-3	210	93	Drilled in 1962; reached water table but insufficient temperature for production; abandoned.
3081-01	Geothermal-4	88.4	43	Drilled in 1962; insufficient temperature for production; abandoned and now plugged.

3×10^6 m^3/mo following the *M*-7.5 earthquake that occurred on the ERZ in 1975 (Dzurisin, 1981). Other studies of surface features such as pit craters (Macdonald and Abbott, 1970; Holcomb, 1980), and of petrologic characteristics of rift eruptions (Swanson and others, 1976; Moore, 1983) indicate that intrusive bodies remain molten for extended periods and may act as subsidiary magma chambers to surface eruptions occurring long after their initial intrusion into the rift zone.

Numerous geophysical studies tend to confirm this interpretation. The total-intensity aeromagnetic map of the rift zone prepared by Godson and others (1981) indicates a clear magnetic signature along the entire length of the rift. This magnetic signature has been interpreted as indicating the presence of temperatures in excess of the Curie temperature of basalt at an estimated depth of 2–3 km (D. Jackson, oral commun., 1985). Controlled-source resistivity surveys on the upper rift have also indicated low subsurface resistivities at depths of 2–5 km, which have been interpreted to be thermal fluids or molten magma bodies (Kauahikaua and others, 1979; Kauahikaua, 1981). More recent very low frequency (VLF) surveys over the ERZ (Flannigan and Long, chapter 39) have similarly identified magnetic and resistivity anomalies that have been inferred to delineate the currently active part of the rift zone and, in some places, molten magma stored in the rift. Although the presence of molten intrusives on the LERZ has not been unequivocally demonstrated, resistivity (Keller and others, 1977; Kauahikaua and others, 1980; Kauahikaua, 1981), self-potential (Zablocki, 1976, 1977), and deep drilling results (Shupe and others, 1978; Yuen and others, 1978; Thomas, 1982) have indicated the presence of high-temperature water.

Although the surface expression of the rift zone is only about 3–4 km wide, some studies suggest that it may be much broader in the subsurface. Swanson and others (1976) analyzed deformation and seismic data for the ERZ and proposed that the focus of active intrusion and eruption on the rift zone has migrated southward with time. Their model considers the north flank of Kilauea to be essentially fixed due to the buttressing effect of Mauna Loa to the north, but that the steep submarine slope to the south of the rift is more mobile and is readily displaced by the forceful intrusion of magma into the rift. The sharp bend in the upper rift is interpreted to be the result of the southward migration of the rift and, on this basis, a subsurface dike complex on the upper rift could approach 10 km in width. Although this width has not been confirmed, interpretations of gravity data by Swanson and others (1976) and gravity and magnetic data by Furumoto (1978) are consistent with a broad subsurface dike complex.

In summary, the structure of the ERZ consists of a broad complex of steeply dipping dikes and fractures extending in a northeasterly direction from the summit caldera for a distance of more than 100 km to the ocean floor. The available geophysical data indicate that the maximum temperatures present at depth in the interior of the rift are in excess of the Curie point. However, the very high permeability of subaerial and shallow submarine extrusive lava is likely to allow rapid hydrothermal circulation and high heat loss rates in the shallow subsurface; hence, only very young intrusives are expected to be significantly above ambient temperatures at depths of less than 1–2 km.

SURFACE HYDROLOGY AND CHEMISTRY

The near-surface hydrology of the ERZ is characterized by very high recharge rates and rapid subsurface ground-water flow. Rainfall rates exceed 2.5 m/yr over most of the ERZ, and the very high permeabilities of the surface volcanic rocks allow nearly 100 percent of the rainfall to penetrate to basal aquifers (Davis and

TABLE 56.2.—*Chemical data from shallow ground-water wells on the lower east rift zone*

Well	Name	Temperature (°C)	pH	Chemical contents (parts per million) Na	K	Ca	Mg	Cl	SO_4	SiO_2	Tritium age[1] (yr)	Na-K-Ca temperature (°C)	$^2SiO_2$ temperature (°C)	$^3SiO_2$ temperature (°C)
2487-01	Keauohana	20.8	7.05	95.1	12.4	15.4	5.1	160	28.6	44.5	18	149	66.1	96.5
2783-01	Malamaki	52.2	7.45	3,333	218	293	295	5,380	598	100.7	15.6	149	111	137.5
2881-01	Allison	37.8	7.35	1,188	68	84	102	2,042	69.2	24.1	12.9	122	39	70.6
2982-01	Geothermal 3	93	6.85	2,572	378	194	122	4,645	314	96.6	10.3	257	108	135
2986-01	Pahoa	23.3	6.65	16.7	9.3	4.5	3.1	4.93	27.3	50	10.6	310	72	102
3080-02	Kapoho	22.1	7.1	127	15	65.6	35.2	174	328	53.6	10.5	124	75	105
3081-02	Airstrip	33.5	7.75	241	28	37.6	27.4	364	211	71.3	11.1	154	91	119

[1]Kroopnick and others, 1978.
[2]Chalcedony.
[3]Quartz conductive cooling.

Yamanaga, 1968). Ground-water transmissivities are typically 5×10^4 darcies (Mink, 1977; Druecker and Fan, 1976) and hence ground-water residence times, as indicated by tritium dating (table 56.2), are typically less than 10–20 years (Kroopnick and others, 1978); discharge of basal fresh water in coastal springs has been estimated at 88–131 m^3/s (Stearns and Macdonald, 1946; Davis and Yamanaga, 1968; Macdonald and others, 1983).

The temperatures and chemical compositions of ground water on the LERZ (table 56.2) span a broad range and suggest that recharge to the basal ground water in this region is received from several very different reservoirs. Four candidate sources could be anticipated in the region: cold, fresh meteoric recharge; cold sea water; hydrothermal fluids of meteoric origin; and hydrothermally modified sea water. The most convenient tracers that can distinguish these possible reservoirs are temperature, chloride-ion concentration, and the chloride-ion:magnesium-ion ratio. Above-ambient ground-water temperatures are clearly indicative of hydrothermal recharge; chloride-ion concentrations permit the identification of fluids of sea-water origin; and, because magnesium has been found to be heavily depleted by hydrothermal processes (Bischoff and Seyfried, 1978; Cox and Thomas, 1979), the chloride:magnesium ratio is able to provide a qualitative indication of the degree of hydrothermal modification undergone by fresh or saline water independent of the measured temperature. A plot of chloride-ion concentration versus temperature and versus chloride:magnesium ratio (fig. 56.2) provides an indication of the relative contributions of the various candidate source fluids to the ground water in the LERZ. Endmember compositions for the candidate sources are plotted for comparison: fresh water is represented by data from well 2986-01, located north of the rift; cold saline fluid by sea water; hydrothermal-meteoric recharge by the early, low-chloride fluids encountered at HGP-A; saline hydrothermal fluids by the fluid compositions found in high-temperature sea water-basalt experiments (Cl:Mg ratio; Seyfried and Bischoff, 1981) and at midocean-ridge hydrothermal systems (temperature).

The distribution of the data points on figure 56.2 suggests the following observations: (1) Chloride concentrations show a broad variation ranging from near fresh-water chloride to almost 30 percent sea-water chloride. (2) The chloride concentrations show a modest correlation with temperature: higher temperature ground water generally has a higher chloride concentration. (3) The degree of alteration of the thermal fluids, as indicated by the Cl:Mg ratio, generally varies and is well below that found in HGP-A or in high-temperature sea water-basalt experiments. (4) The Cl:Mg ratio is not well correlated with either temperature or chloride concentration: well 2982-01 shows a high temperature and high chloride concentration and a moderately depleted magnesium concentration (relative to sea water), well 2783-01 shows intermediate temperatures, high chloride, and only minor magnesium depletion, and well 2487-01 shows a low temperature and low chloride concentration but a significant magnesium depletion. These observations suggest that meteoric recharge is the predominant source for ground water in the region. However, sea water that has undergone varying degrees of hydrothermal alteration contributes as much as 30 percent

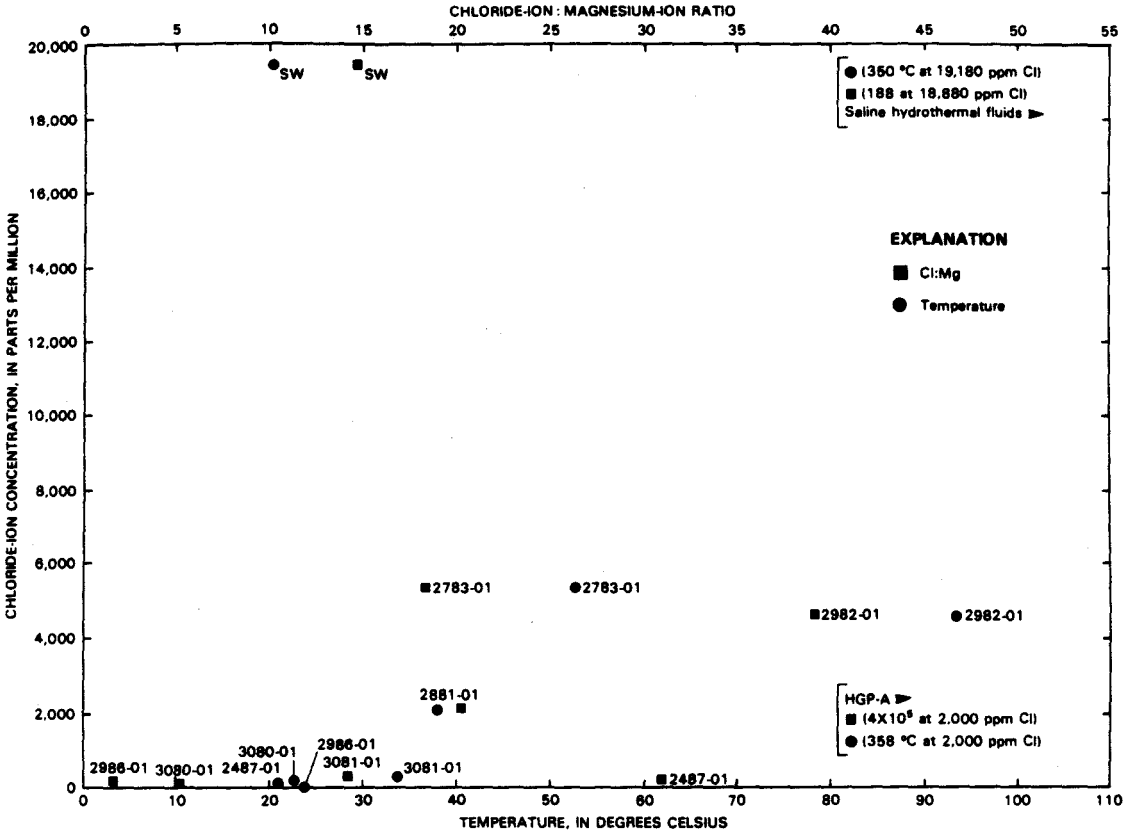

FIGURE 56.2.—Chloride-ion concentration versus temperature and versus chloride:magnesium ion ratio in shallow ground-water wells on lower east rift zone. Wells are identified by number (see fig. 56.1). Data from well 2986-01 represent fresh water; HGP-A data represent hydrothermal-meteoric recharge from early, low-chloride-ion fluids from HGP-A; saline-hydrothermal-fluid data represent high-temperature sea water-basalt experiments (Cl:Mg ratio) and midocean-ridge hydrothermal systems (temperature); SW, sea water.

of the recharge to the basal lens. The role of high-temperature, heavily modified, fresh and saline water in the basal aquifers is not as clearly defined. The chemistry of well 2487-01 could be modeled as a mixture of fresh ground water with a small addition of low-salinity, heavily altered hydrothermal fluid. The low temperatures suggest that the contribution from the latter source is, however, very small.

As many as four source fluids appear to have an influence on the ground-water temperatures and chemical compositions on the LERZ:meteoric recharge; cold, relatively unaltered sea water; higher temperature altered sea water; and low-salinity, heavily altered hydrothermal fluid.

The mixing of these multiple-source fluids in the shallow ground-water aquifers renders any attempt to apply chemical geothermometers highly suspect. Temperatures calculated using the Na-K-Ca geothermometer (Fournier and Truesdell, 1973; Fournier, 1981) are generally correlated with measured temperatures (table 56.2) although the correlation is far from uniform. The silica geothermometer (Fournier and Potter, 1982) similarly yields varying apparent temperatures that, although generally correlated with measured temperatures, do not yield significant insight into the deeper reservoir.

The rate of convective discharge of the thermal energy from the interior of the rift can be crudely estimated using the data from the shallow wells and assuming that: (1) the mean ground-water temperature of the aquifer south of the northern boundary of the ERZ and east of well 2487-01 is the average of that found in wells 2783-01, 2881-01, 3081-01, and 2982-01; and (2) the rate of fresh-water recharge is equivalent to the average rainfall rate in this area. Using these assumptions, the mean ground-water temperature is calculated to be about 54 °C. The average rainfall rate is approx-

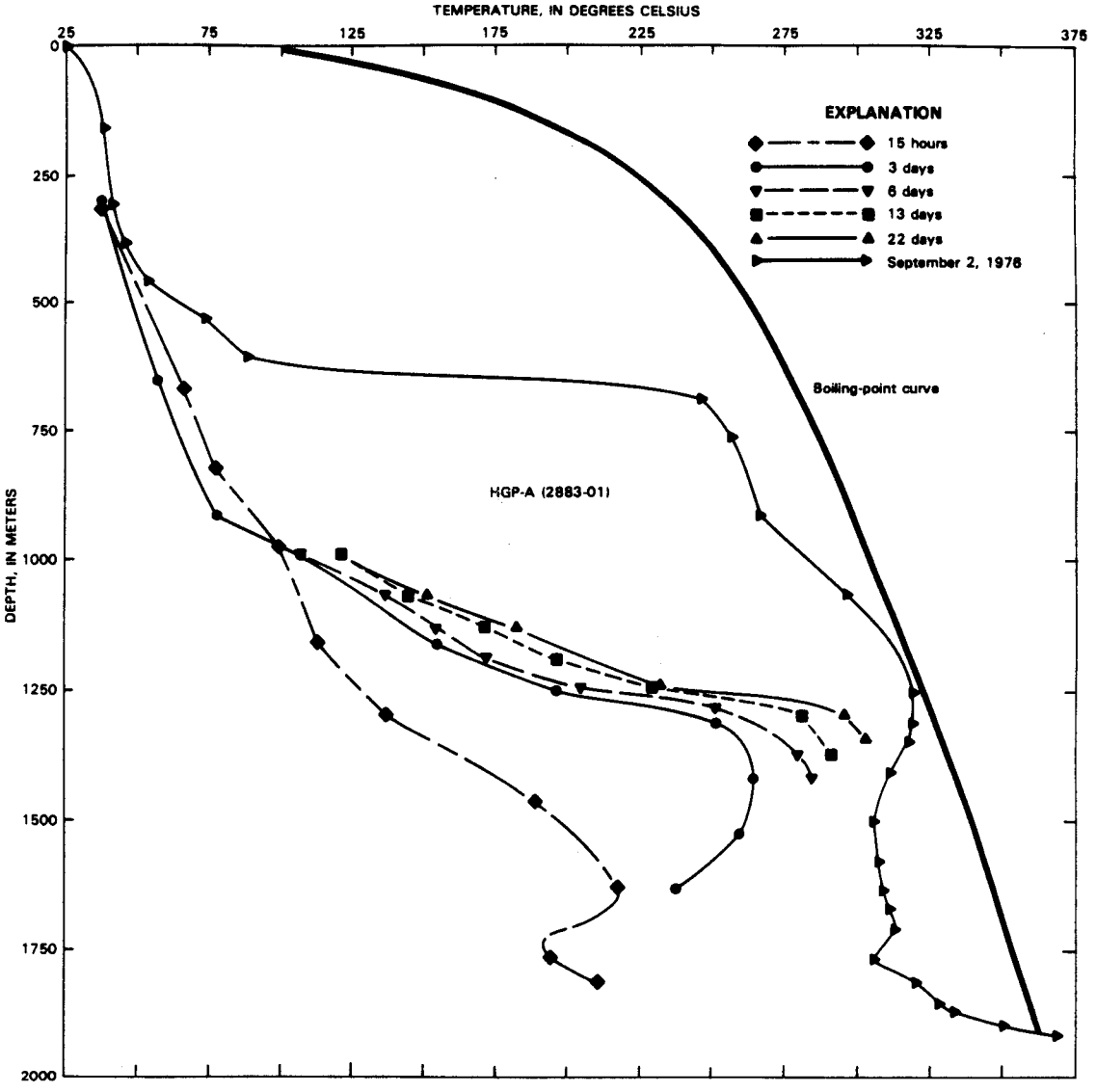

FIGURE 56.3.—Downhole temperatures measured in well 2883-01, HGP-A geothermal well. Individual curves reflect downhole temperature measurements made at specified times after mud circulation in well was suspended. Profile for 9/2/76 was measured with water in borehole.

imately 2.5 m/yr and the area of interest is approximately 25×10^6 m^2; thus, the total fresh-water recharge is approximately 62.5×10^6 m^3/yr. Hence the total thermal discharge in this limited region is estimated to be a minimum of 2.19×10^{12} kcal/yr or approximately 291 megawatts of thermal energy continuously. If this heat loss rate is extrapolated over the subaerial rift zone, 50 km of rift zone versus 10 km in the area of the thermal discharge, the heat loss would be approximately 1,455 thermal megawatts. The magma intrusive rate estimated by Dzurisin (1981) at 3×10^6 m^3/mo would bring an estimated 2,800 thermal megawatts into the rift zone. In light of the approximations made and the very short timespans considered, these values are in remarkably close agreement and may be interpreted to

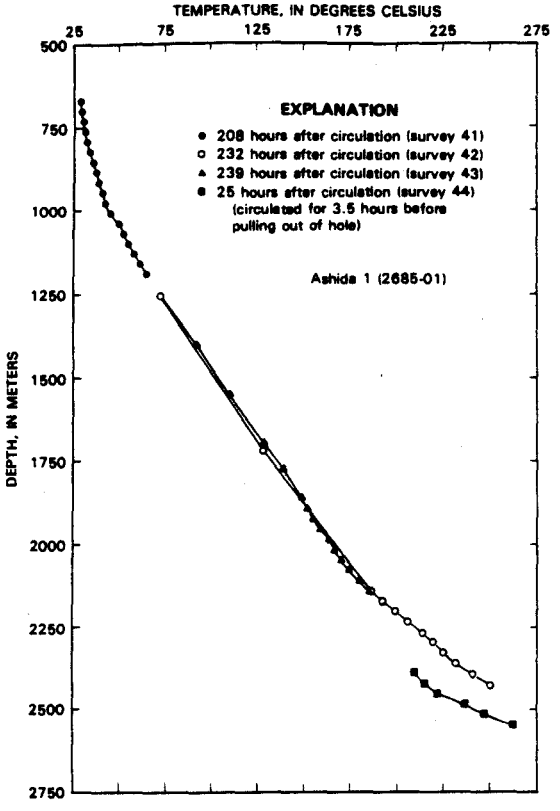

FIGURE 56.4.—Downhole temperatures measured in well 2685-01, Ashida 1.

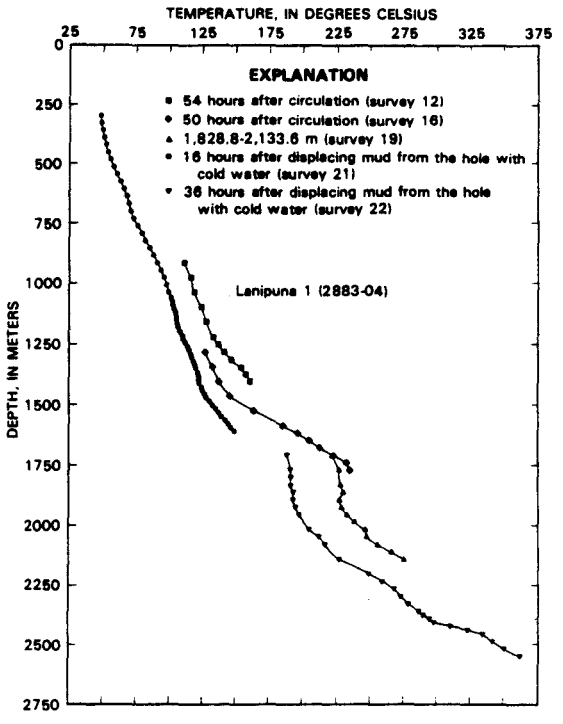

FIGURE 56.5.—Downhole temperatures measured in well 2883-04, Lanipuna 1.

indicate that the rates of convective heat loss to the shallow hydrologic system nearly balances the heat recharge from magmatic processes. If this interpretation is correct, it would in turn suggest that the residual heat present in a rift zone after cessation of intrusive activity would decrease very rapidly.

DEEP HYDROLOGY

The HGP-A well, completed in 1976, was the first deep research well drilled into the ERZ; seven privately funded deep wells have been completed subsequent to HGP-A in an effort to further define the geothermal resource discovered by this well. HGP-A was funded by several public and private agencies (the U.S. Department of Energy, National Science Foundation, State of Hawaii, County of Hawaii, and Hawaiian Electric Company), and hence more data for this well is publicly available than for the privately financed exploration wells. However, sufficient data has been released to allow us to permit limited extrapolation of the HGP-A data to other parts of the ERZ.

THERMAL CHARACTERISTICS

The available data from all the deep geothermal wells presently drilled in the LERZ are presented in table 56.1. All but two of the wells recently drilled penetrated to a depth of 2,000 m. The maximum temperatures encountered in each well were substantially above the normal geothermal gradient found in Hawaii. However, clear differences are present in the maximum temperatures encountered in each well, and examination of the temperature profiles is especially revealing. The temperature profiles used for each well must be interpreted carefully however: temperatures measured immediately after drilling and mud circulation cease are likely to be below equilibrium temperatures, whereas those measured after mud has been cleared from the hole may be affected by water circulation within the wellbore. The conditions under which the profiles were taken, if known, are noted.

The well profiles (figs. 56.3–56.6) generally show a shallow zone of moderate temperature over the first 500–1,000 m of the well. The moderate and relatively uniform temperatures in this interval reflect high meteoric recharge rates and rapid ground-water circulation and mixing in the very permeable subaerial and shallow submarine basalts. Underlying this zone is an interval of gradually

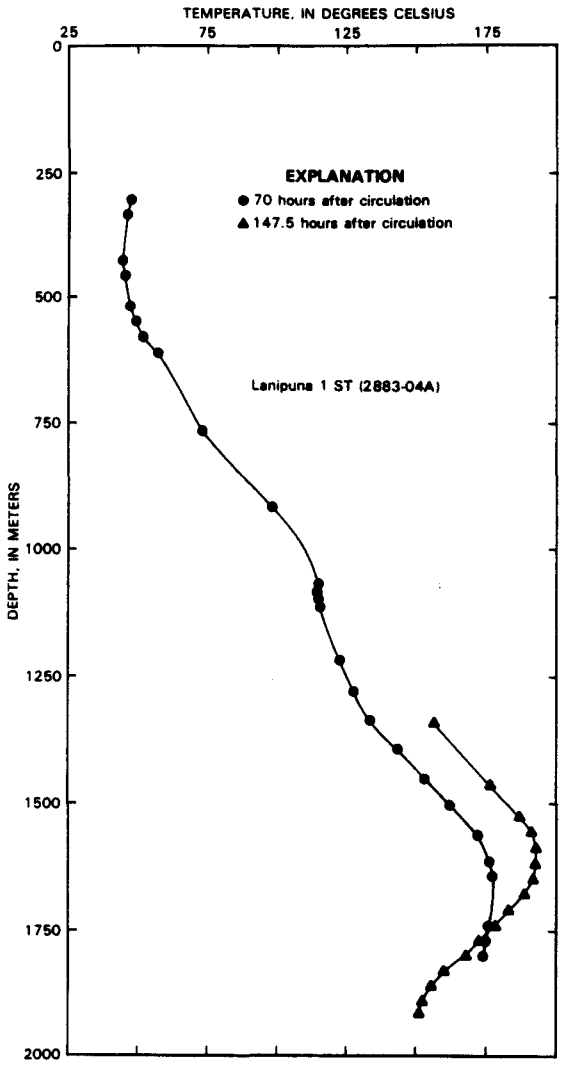

FIGURE 56.6.—Downhole temperatures measured in well 2883-04A, Lanipuna 1 side track.

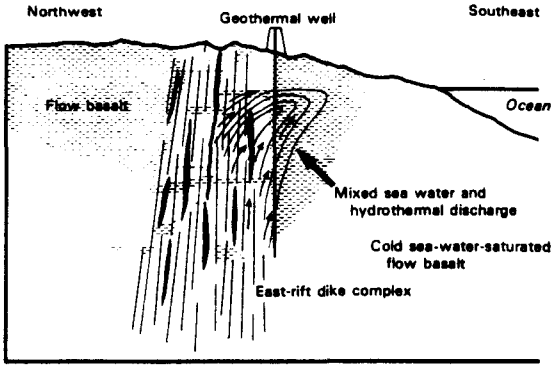

FIGURE 56.7.—Conceptual cross section of lower rift showing fluid circulation across rift zone. Thermal waters, exiting rift toward southeast, form a tongue of hot water overlying colder fluids below. Drilling on southern edge of rift would initially encounter thermal fluids at shallow depths, but at greater depths would reenter lower temperature aquifers.

increasing temperature, possibly representing a conductive temperature gradient, that indicates the decline in basalt permeability and a reduction in the rate of hydrothermal circulation. Below the conductive region, the temperature gradient may steepen and approach a curve corresponding to the temperature of steam-saturated water under hydrostatic pressure (the boiling curve). The conformance to the boiling curve suggests that the thermodynamic conditions in the deep reservoir are controlled by hydrostatic pressure and not by physical barriers, such as a reservoir cap rock. There are, however, exceptions to this general trend. The data from wells 2883-04A and 2883-05 show a distinct temperature turnover in the lower portions of both holes. The location of these wells on the southern boundary of the rift suggests that the wells may have passed through a reservoir outflow zone and penetrated into colder aquifers below (fig. 56.7). This interpretation leads to the speculation that the fractures and intrusives on the southern edge of the ERZ dip toward the north. If the rift structure had a southward dip, deeper drilling in this location would be anticipated to penetrate toward higher temperature intrusives.

A comparison of the temperature distribution among the wells and their relative locations shows that the maximum temperatures encountered are very site specific. For example, well 2883-04 encountered a bottom-hole temperature of >368 °C, the highest temperature reported for the LERZ wells, but a redrill of this well (2883-04A), completed as a slant-hole offset, encountered maximum temperatures of only 193 °C with a bottom-hole temperature reversal (figs. 56.5 and 56.6). The bottom of the redrill is less than 500 m from the bottom of its original straight configuration and from HGP-A, yet its peak temperature is more than 160 °C below the maximum temperatures encountered in either well. The temperatures encountered along the southern boundary of the ERZ vary greatly and may be strongly influenced by local hydrologic conditions. Although fewer wells have been drilled on the interior of the ERZ, the reported temperature information indicates somewhat more consistency than is found on its edge (Iovanitti and D'Olier, 1984).

PETROLOGY

The petrology of the rocks encountered in the deep exploration wells has not as yet been analyzed in detail. HGP-A was the only well from which cores were taken and hence is the only well for which bulk rock analyses can be done. However, analyses of the cuttings that have been released from the other wells (Barnwell

Geothermal Corp., unpublished data, 1985) are very informative as to the type of alteration present. The wells for which preliminary analyses are available include HGP-A, 2685-01, 2883-04, 2883-04A, and 2883-05; although analyses have been completed for wells 2883-02 and 2883-03, the data have not been released, and a second analysis is currently underway for archived samples from well 2883-02.

Samples of the cuttings from all of the wells indicate the presence of basalt throughout the section. The morphology of the basalt ranges from highly vesicular in the shallow subsurface to dense, nonvesicular pillow lava and dike rocks at depth. Hyaloclastites, palagonitized ash, and hematite were found at depths of 500–800 m below ground level and approximately 300–500 m below the current sea level (Stone, 1977; Barnwell Geothermal Corp., unpublished data, 1985). The morphology and oxidation of the basalt may indicate the approximate location of sea level at the time of extrusion of the lava. Rock textures range from aphyric glass, associated with chill margins or pillow lava, to olivine-phyric and plagioclase-phyric lavas.

The alteration mineralogy found in the individual wells follows a relatively consistent pattern. The shallow parts of the wells are typified by mild low-temperature alteration and deposition products such as montmorillonite clays, anhydrite, and calcite (Stone, 1977; Stone and Fan, 1978; Waibel, 1983). As the depths and temperatures increase, the degree of alteration generally increases as does the grade of metamorphism. Trends in the mineral suites show incipient alteration at intermediate temperatures that increases to total replacement of parent minerals by chlorite and lesser amounts of accessory products such as albite or, at the highest temperatures, epidote (figs. 56.8–56.11). In addition to the above, other alteration products found throughout the geologic section include calcite, anhydrite, zeolites, quartz, pyrite, and magnetite. Despite these general trends, the degree of alteration is by no means continuous throughout the section. Alteration is intermittent, and the extent of alteration at a given depth and temperature varies greatly, thus implying that the alteration process is highly dependent upon the access of (saline?) fluids to the interior of the rift. This intermittent alteration in turn suggests that, whereas temperature is the primary controlling factor in the alteration of the basalt, fracture permeability and fluid circulation within the rift are also major factors.

The depths of the various alteration minerals are significant to the model of hydrothermal circulation within the ERZ. As noted above, anhydrite is distributed throughout the cuttings from some wells and is apparently confined to only a few depth intervals in others. The retrograde solubility of anhydrite and the presence of relatively high concentrations of calcium and sulfate in sea water suggest that anhydrite is being deposited from sea water circulating within the ERZ. Laboratory studies of sea water-basalt reactions have shown that calcium sulfate is removed from sea water as anhydrite (Mottl and Holland, 1978; Mottl and Seyfried, 1980; Seyfried and Mottl, 1982) and that nearly quantitative removal of calcium occurs before temperatures reach 225 °C. The presence of anhydrite in both the low-temperature and the higher temperature parts of the rift could be accounted for by either of two possible

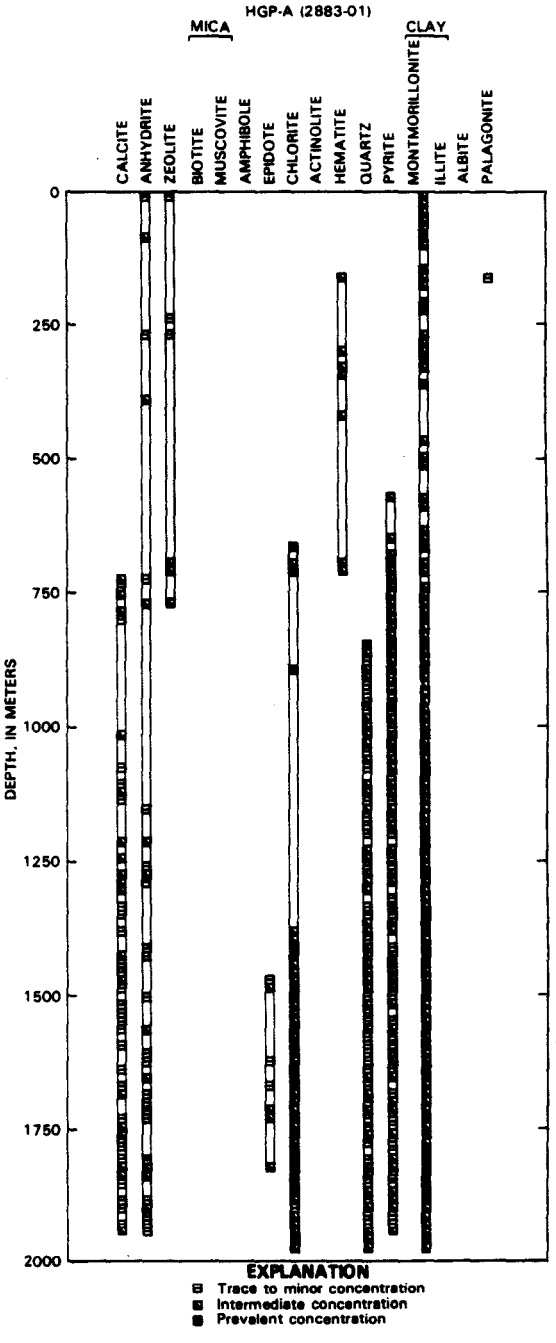

FIGURE 56.8.—Alteration mineral suites encountered with depth in HGP-A. (From Columbia Geosciences, unpublished data, 1983.)

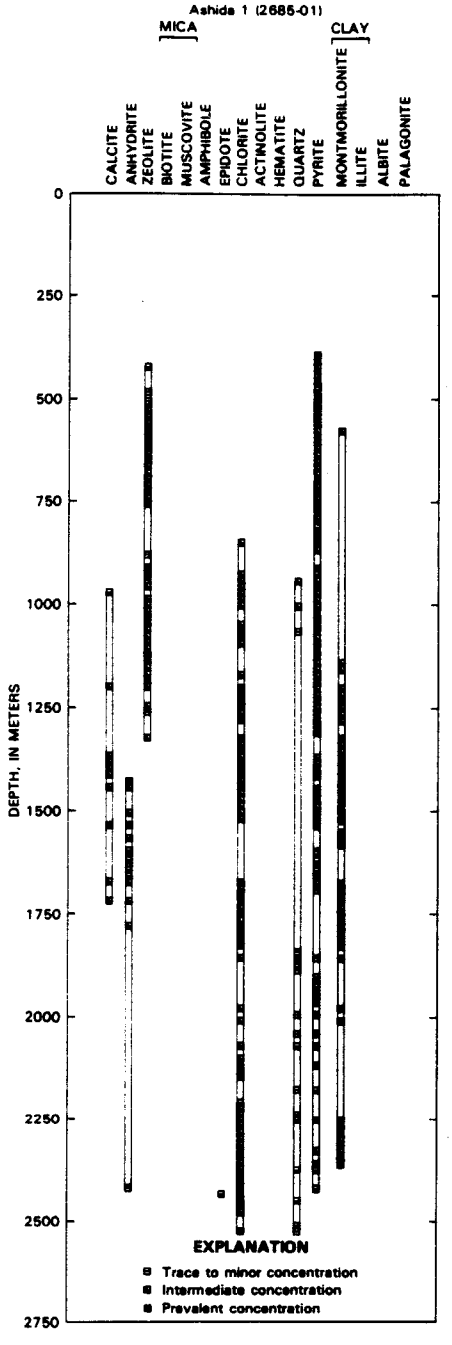

FIGURE 56.9.—Alteration mineral suites encountered with depth in well 2685-01. (From Barnwell Geothermal Corp., unpublished data, 1985.)

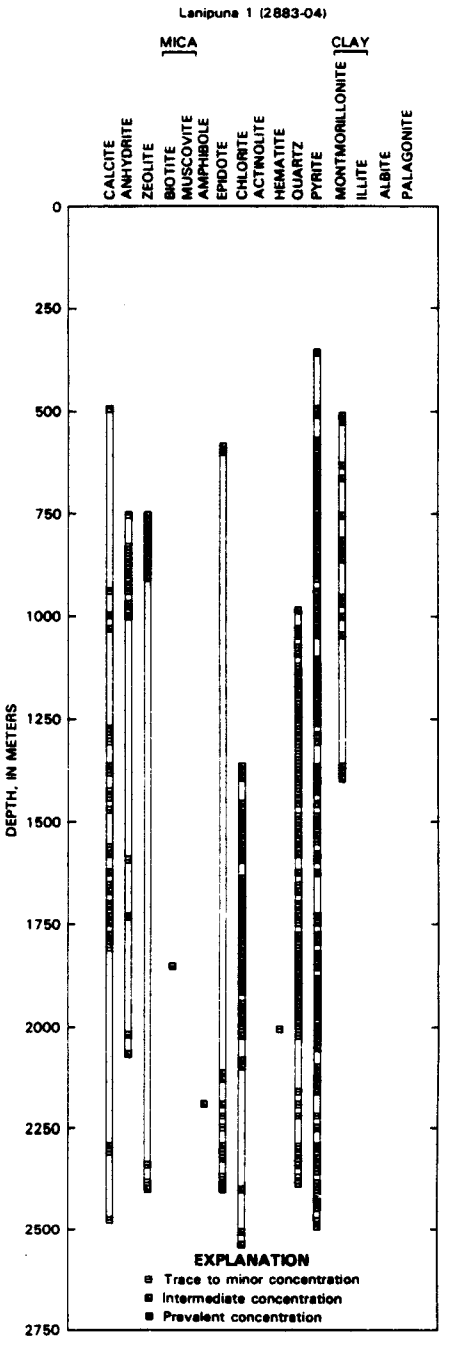

FIGURE 56.10.—Alteration mineral suites encounterd in well 2883-04. (From Barnwell Geothermal Corp., unpublished data, 1985.)

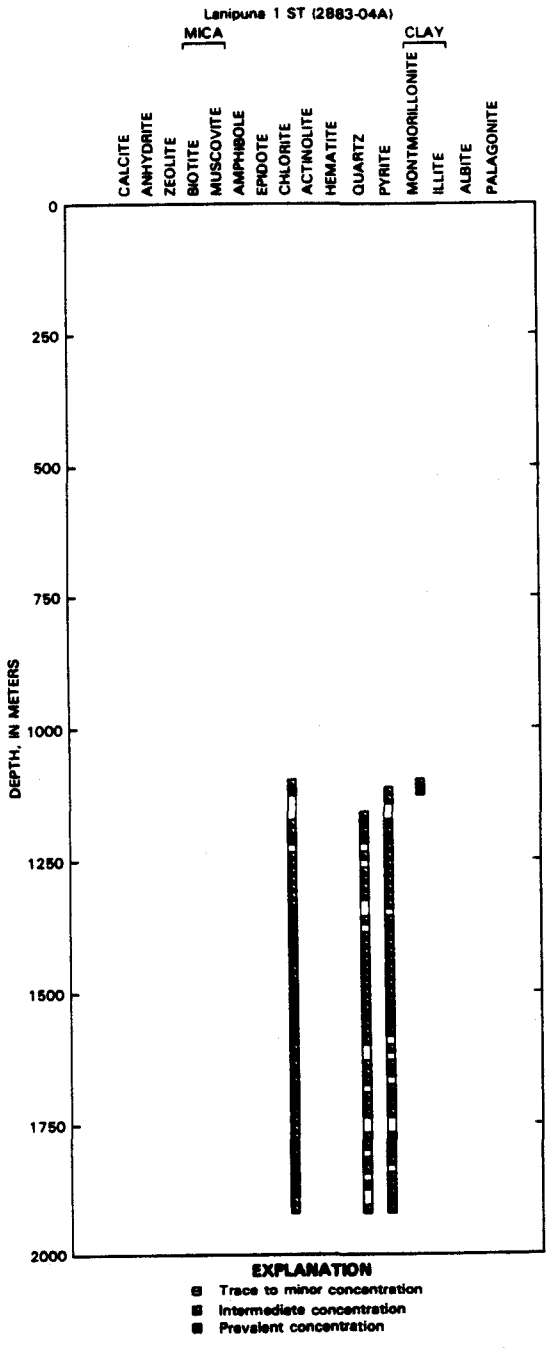

FIGURE 56.11.—Alteration mineral suites encountered in well 2883-04A. (From Barnwell Geothermal Corp., unpublished data, 1985.)

mechanisms: (1) anhydrite precipitation continues at higher temperatures as calcium is mobilized from the basalt matrix by hydrothermal alteration; (2) the part of the rift penetrated by these wells has undergone a complex history of heating and cooling associated with successive episodes of magmatic intrusions and subsequent cooling by hydrothermal circulation.

Pyrite and quartz are present throughout virtually the entire section below sea level. Due to the low temperatures and low metamorphic grades present in the shallow parts of the wells, the fluids precipitating these minerals probably did not originate at the depths of deposition, and hence they represent deposition from cooling hydrothermal fluids discharged from deeper within the rift.

Minerals found in the altered parts of the deep wells are quite similar to those found in sea water-dominated hydrothermal systems such as Reykjanes (Tomasson and Kristmannsdottir, 1972; Kristmannsdottir, 1976), in dredge samples from sea-floor spreading centers (Humphris and Thompson, 1978), and in laboratory studies of sea water-basalt reactions at high temperature (Mottl and Seyfried, 1980; Seyfried and Mottl, 1982). Clearly, the primary agent responsible for the alteration mineral suite observed is the intrusion of sea water into the interior of the ERZ. However, because the grade and intensity of hydrothermal alteration in each well varies with depth, the intermittent highly altered zones in the reservoir are interpreted to be the result of fracture-mediated intrusion of sea water into the interior of the rift.

PRODUCTION CHARACTERISTICS

The production characteristics of the individual wells have varied over a broad range. HGP-A initially produced a mixed-phase flow comprised of approximately 50 percent steam and 50 percent liquid, at approximately 45,000 kg/h. Discharge rates increased slightly during testing and, at the beginning of production for the HGP-A generator facility, amounted to approximately 50,000 kg/h. The steam:brine ratio is a function of wellhead pressure and, at the operating pressure of the facility, is approximately 57 percent liquid and 43 percent steam at a pressure of 1,200 kPa. Production from the well showed a gradual decline over the first 40 months of operation of the generator facility amounting to about 10–15 percent of its total output. However, during a 48-hour period on the fortieth month, wellhead pressures and production rates increased by slightly more than was lost during the prior forty months. The change occurred in distinct steps that were not accompanied by any seismic activity and hence were probably the result of a change in the wellhole, such as the elimination of an obstruction. This interpretation suggests that the total production from HGP-A may be limited by the borehole diameter rather than by the inherent productivity of the reservoir.

Analysis of the changes that have occurred in the production chemistry indicates that HGP-A is producing from two separate reservoirs having very different characteristics. The liquid or brine phase is apparently produced from an intermediate-depth reservoir having a temperature of approximately 260–280 °C, whereas dry-steam production is occurring from near the bottom of the well.

TABLE 56.3.—*Summary of HGP-A liquid-phase chemistry*

Date	Depth/ pressure	Chemical contents (parts per million) Na	K	Ca	Mg	Cl	SO_4	SiO_2	Na-K-Ca[1] temperature (°C)	Quartz[2] temperature (°C)	Water:rock ratio ([3])	([4])
12/2/76	1,300 m	480	85	17.3	0.7	920	--	740	262	290	3.2	0.71
2/9/77	103 kPa	720	135	30.1	.1	1,610	--	--	219		3.7	.81
4/22/77	103 kPa	1,480	277	72.2	.1	3,190	--	--	298		3.5	.77
1/16/80	910 kPa	1,520	224	33.9	.01	2,593	69	832	278	303	3.5	.78
6/12/81	103 kPa	900	200	25.5	.008	2,065	--	1,198	336	296	3.1	.67
9/4/81	1,200 kPa	1,890	295	66.5	.029	3,622	--	860	281	307	3.8	.84
12/11/81	103 kPa	1,590	300	33	.012	2,763	--	1,004	332	280	2.6	.58
6/7/82	1,170 kPa	3,120	525	122.5	.051	5,667	--	803	309	299	3.2	.71
11/16/82	1,170 kPa	3,940	650	217	.104	7,029	--	829	301	303	3.2	.71
5/4/83	1,170 kPa	4,220	675	270	.152	7,965	--	805	292	300	3.6	.80
12/5/83	1,100 kPa	4,650	763	319	.210	8,827	24	825	298	303	3.5	.77
6/26/84	1,100 kPa	4,840	773	489	.25	8,900	15	885	282	310	3.5	.77
11/28/84	1,100 kPa	5,420	733	399	.20	9,514	4.5	913	265	314	4.12	.91

[1]Fournier, 1981.
[2]Fournier and Potter, 1982.
[3]Water to rock ratio based on original sea-water potassium concentration of 399 ppm and Kilauea tholeiite average concentration of 4,500 ppm, and a potassium removal efficiency of 100 percent.
[4]As above but using an extraction efficiency of 22 percent (Seyfried and others, 1984).

The production characteristics of the other geothermal wells on the LERZ have not been as well characterized as that from HGP-A; however, the data available indicate widely divergent discharge patterns. Short-duration production tests conducted on three wells north of HGP-A (2883-02, 2883-03, 2883-06) have clearly confirmed the presence of dry-steam production from the LERZ reservoir: two of these wells initially produced a mixed phase of steam and water that changed to dry steam over a period of a few hours (Iovanitti and D'Olier, 1984). The production rates from the first two wells were reported to be 15 t/h and 33 t/h, respectively; however, the duration of the tests conducted and the presence of debris in the hole suggest that these are neither equilibrium nor representative flow rates. (This third well, 2883-06, was also productive; however, the engineering data are presently confidential.)

In contrast to the wells located north of HGP-A, three of the wells drilled on the southern boundary of the rift (2883-04, 2883-04A, and 2685-01) were unable to sustain production at all. Although permeable zones, as indicated by drilling-mud-loss records, were encountered in these wells, the available records indicate that the permeable zones were much more limited south of the rift than at HGP-A or in the wells more interior to the rift. The fourth well, 2883-05, encountered an extremely permeable fracture at a depth of approximately 1,600 m that did not have sufficient temperature to sustain production.

RESERVOIR CHEMISTRY

The HGP-A well is the only deep well in the LERZ for which a significant number of samples have been analyzed, and hence the data set from HGP-A yields the most complete picture of the chemical processes underway in the hydrothermal system associated with the ERZ. The limited data set available from the other wells is, however, consistent with the model derived from HGP-A.

The composition of the fluids produced by HGP-A during its production life has shown complex changes during each period of discharge and between periods of discharge. Samples obtained from downhole samplers and from production fluids taken immediately after well completion showed very low dissolved solids concentrations (table 56.3); chloride levels generally ranged from about 1,000 mg/kg to 2,000 mg/kg whereas the total-solids content was approximately 3,000 mg/kg to 5,000 mg/kg. Subsequent samples of discharge fluids showed an increase in the salinities during each well test but a slight reduction in chloride concentrations between tests. The rate of increase during the first production tests was relatively rapid; initial chloride concentrations of approximately 1,000 mg/kg in the liquid phase increased to more than 2,000 mg/kg after steam production (flashing) began and continue to increase throughout the period of discharge. The longest test period, prior to the installation of the generator facility, spanned 1,000 hours; the chloride concentration in the brine at the conclusion of that test was approximately 3,200 mg/kg.

Downhole sampling during the preliminary testing provided chemical data indicating that production was occurring from at least three aquifers: one at a depth of approximately 700 m produced cold saline water; a second at a depth of approximately 1,500 m produced low-salinity fluids; and a third at a depth of approximately 1,900 m produced low- to intermediate-salinity fluids (Kroopnick and others, 1978). Although a subsequent recasing program sealed off the cold, high-salinity aquifer, continuous discharge of fluids from HGP-A between 1983 and 1985 continued to generate substantial increase in salinity (fig. 56.12); by the end of 1985 after four years of continuous production, the chloride concentrations reached a level of approximately 10,000 mg/kg.

The other major dissolved solids present in the brine phase include sodium, potassium, calcium, and silica. The concentrations of all but the latter have shown increases similar, although not

identical, to those observed for chloride (table 56.3). Silica concentrations in the brine have shown little if any verifiable change beyond those associated with changes in the power plant operating conditions.

In contrast to the evolution of the brine chemistry, the gases present in the steam phase have shown very modest variations. Although the gas-chemistry data obtained from HGP-A during the preliminary well testing are suspect due to analytical and sampling difficulties, the data indicate that the major gases, CO_2 and H_2S, were present at concentrations of less than 1 percent by weight of the steam. Subsequent analyses, conducted during power plant operations, determined that the concentrations of the major gases were approximately as follows: CO_2, 1,250 mg/kg; H_2S, 950 mg/kg; N_2, 130 mg/kg; H_2, 12 mg/kg; and CH_4, 1 mg/kg. Changes in the gas concentrations were observed during the initiation of well flow that correspond to stabilization of the reservoir in response to production, but subsequently they declined at a very modest rate during the three and one-half years of power plant operations. The gas concentrations currently amount to: CO_2, 1,150 mg/kg; H_2S, 850 mg/kg; N_2, 120 mg/kg; and H_2, 12 mg/kg.

Although the chemistry data available from the other privately financed geothermal wells is quite limited, the following information has been made available: Wells 2883-04 and 2883-04A, located on the southern boundary of the rift zone, encountered fluids having salinities approximately equivalent to sea water in the permeable, intermediate-temperature parts of the holes. Due to inadequate permeability at depth, these wells were unable to produce steam or a high-temperature mixed phase. Wells 2883-02 and 2883-03, north of HGP-A, produced fluids having dissolved-solids concentrations of a few thousand milligrams per kilogram to near the solids saturation point, depending upon the wellhead pressures and steam qualities during the production tests. Reported total gas concentrations were approximately 2,000 mg/kg of which 1,100 mg/kg was H_2S (Iovanitti and D'Olier, 1984). Testing of the private exploration wells indicated that multiple production zones were encountered in all wells, and hence the precise source for the fluids are known only to the extent that they are derived from a depth greater than the casing depth of the wells or about 1,100 m below sea level.

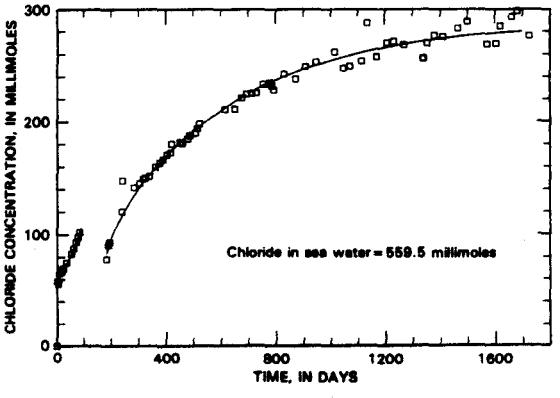

FIGURE 56.12.—Chloride concentrations in brine phase from HGP-A versus duration of production. The interval from day 84 to day 183 represents a period from September 4, 1981, to December 11, 1981 when flow from the well was suspended.

DISCUSSION OF CHEMICAL DATA

One of the most striking aspects of the fluid chemistry data from HGP-A is the very low salinities encountered at depth immediately after well completion. This result was not anticipated, and the presence of fresh water at depth was initially attributed to the presence of drilling fluids lost to the deep production aquifers. However, analysis of tritium levels present in surface waters used for drilling and those from the reservoir (Kroopnick and others, 1978) conclusively demonstrated that the early reservoir fluids were not contaminated by recent surface water. Subsequent analyses conducted after an extended flow test of the well reconfirmed the absence of significant tritium activity in the reservoir fluids (Thomas, 1980).

Because of the density difference between fresh and saline water, the Ghyben-Herzberg model, typically used to describe ground-water hydrology in an island environment predicts that a fresh-water lens should be found floating above sea water in the basal aquifers. The thickness of this lens is dependent upon rainfall recharge rates and the effective permeability of the basal aquifers; in the vicinity of HGP-A, a lens thickness of approximately 70 m would be predicted. However, the presence of a heat source in the ERZ invalidates one of the major assumptions of the Ghyben-Herzberg model: that a density difference exists between fresh and saline water. With a heat source present in the ERZ, sea water entering the hydrothermal system and heated to reservoir temperatures will have a density less than that of cold fresh water. Thus, cold rainfall recharge can enter the ERZ from above and displace warmer, less dense saline water entering the ERZ laterally. This factor alone probably cannot account for the exceptionally low salinities observed at depth in the reservoir: cold saline water should exert a higher hydrostatic pressure on the reservoir than cold fresh water if the hydraulic head heights and permeabilities of the respective infiltration pathways are equal. Hence, other factors may play a key role in the near exclusion of sea water from the deep hydrothermal reservoir. As discussed above, the rift consists of near-vertical tabular dikes and fractures trending in an east-west direction. Hydrologic studies (Stearns and Macdonald, 1946; Takasaki, 1978; Macdonald and others, 1983) have shown that the permeability of intrusive materials may be several orders of magnitude lower than normal country rock, and therefore, the permeability of the rift zone transverse to its strike should be very much lower than the surrounding rocks outside the dike complex. The presence of fractures parallel to the intrusives serves to further increase the permeability of intervening extrusive rocks within the dike complex. Hence, the structure of the ERZ increases the naturally existing east-west and vertical permeability to fresh-water recharge to the rift but inhibits the entry of sea water from the south due to the lower transverse permeability of the dike system.

A third factor that may play a role in the exclusion of sea water from the ERZ is the reaction sequence undergone by sea water when it is heated to reservoir temperatures. Extensive studies conducted on sea-water chemistry at elevated temperatures (Bischoff and Dickson, 1975; Mottl and Holland, 1978; Bischoff and Seyfried, 1980; Seyfried and Mottl, 1982; Pohl and Liou, 1983) have demonstrated that, when sea water is heated in the presence of basalt, a number of reactions occur that can substantially alter the chemical composition of the sea water and the mineral suites present in the rock. Most pertinent to the present analysis are the findings that: (1) the retrograde solubility product of calcium and sulfate ions in sea water result in anhydrite deposition (Mottl and Seyfried, 1980), and (2) reactions at temperatures of 300 °C result in the devitrification of basalt glass and the breakdown of the common basalt minerals and result in the deposition of smectites, chlorite, wairakite, and other alteration products. One sea water-basalt experiment (Pohl and Liou, 1983) was conducted in a flow-through cell that reportedly became plugged due to alteration mineral deposition in less than 48 hours. Similar reactions occurring in the natural sea water-basalt hydrothermal system on the ERZ may result in a sequence of fracture-induced permeability and subsequent sealing by deposition of alteration minerals along the southern (seaward) boundary of the rift. The presence of anhydrite, deposited as a vein-filling mineral, and of intermittent zones of intensely altered but low-permeability basalt in the cuttings from the deep geothermal wells on the LERZ tend to further substantiate this process. Thus the initial absence of sea water in the reservoir fluids encountered by HGP-A can be accounted for by the inhibition of sea-water recharge into the high-temperature part of the rift by permeability barriers imposed by the dike complex, self-sealing by alteration mineral deposition from hydrothermally heated sea water, and the more rapid recharge of cold meteoric water along highly permeable vertical fractures within the rift.

The increasing trend of dissolved solids in the fluid phase produced by HGP-A was initially interpreted to indicate that fluid withdrawal from a single-phase low-salinity aquifer had generated an expanding zone of boiling around the borehole (Thomas and Sakai, 1983). This model postulated that migration of the boiling front into the reservoir led to a progressively steam-depleted (and solids-enriched) residual brine phase entering the borehole. However, this model also required a progressive decline in the relative volume of brine to steam as the boiling front advanced into the reservoir. The more than fivefold increase in dissolved solids in the HGP-A brines, however, have not been accompanied by a similar decrease in the brine:steam ratio. Hence, the single-production-zone model has been abandoned in favor of a multiple-production hypothesis in which at least two separate production zones are supplying fluids to the well: one aquifer supplying a higher temperature steam phase and a second supplying intermediate-temperature brine and steam.

Other data supporting this model include the gas concentrations present in the HGP-A steam and the reported production characteristics of other wells in the LERZ. As noted above, the concentrations of noncondensable gases present in the HGP-A steam have changed only slightly during the production history of the well. A single production zone undergoing progressive boiling should show a rapid decline in the noncondensable gas concentration present in the steam due to the strong partitioning of the dissolved gases in the steam phase. The near constancy of the gas concentrations in the steam phase thus substantiate multiple, independent production aquifers. Further support for the production of brine and steam from separate aquifers in HGP-A comes from the production characteristics of wells 2883-02 and 2883-03. Both wells are drilled and cased to greater depths than HGP-A and both produced a single-phase steam flow within hours of the beginning of their flow tests. Thus the reservoir on the LERZ is clearly capable of producing dry steam. The absence of a brine phase in the more recently completed wells is attributed to their having been cased to greater depths than HGP-A and thus having excluded lower temperature production aquifers.

The steam-production zone present in HGP-A and other wells on the LERZ is not, however, identical to the more classic dry-steam reservoirs found at The Geysers, California, and Larderello, Italy. The latter have lower equilibrium temperatures and are significantly underpressured: the pressure within the steam zone is less than hydrostatic pressure at equivalent depths, indicating that porosity within the reservoir is filled with a low-density two-phase fluid probably consisting of steam and liquid water (Fournier, 1981). The reservoir temperatures in the deeper parts of the ERZ have generally been much higher than those found at The Geysers and at Larderello and, in the high-temperature wells, follow the boiling temperature versus hydrostatic pressure curve with depth. Wellhole-circulation and wellhead-pressure patterns during shut-in (when there is no well discharge at the surface) indicate that reservoir pressures are sufficient to maintain circulation from deeper permeable zones to shallow discharge points in the uncased parts of the roles. Even though dry-steam production is occurring from the deep reservoir, a single-phase fluid is believed to be present at depth that, because of the high temperature and low permeability in the reservoir, boils entirely to steam prior to entry into the wellhole.

The increased salinity of the liquid phase produced by HGP-A is believed to be the result of sea-water intrusion into the reservoir. No other source of chloride ion of sufficient magnitude to account for the observed changes exists in the Hawaiian environment (evaporites, sediment basins, and so forth) and the sodium:chloride ratio in the fluids is nearly identical to that for sea water (fig. 56.13). However, comparison of the chemical composition of the brines with that of sea water indicates that a substantial modification of the sea-water chemistry has occurred: potassium and calcium have been heavily enriched, whereas magnesium and sulfate have been heavily depleted (table 56.3; figs. 56.14–56.16). These chemical alterations are virtually identical to those observed in laboratory sea water-basalt reaction studies and in fluids discharged from mid-ocean-ridge hydrothermal systems. In very general terms (for more detailed discussion see, Mottl and Seyfried, 1980; Reed, 1982; Seyfried and Mottl, 1982; Mottl, 1983), the sequence of reactions found to occur in hydrothermal sea water is characterized by an initial loss of calcium ion to the deposition of anhydrite, the removal

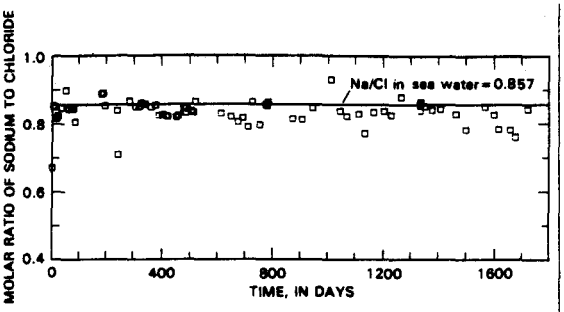

FIGURE 56.13.—Sodium-ion to chloride-ion ratio in HGP-A brines versus duration of production. Straight line represents sodium-ion to chloride-ion ratio in sea water.

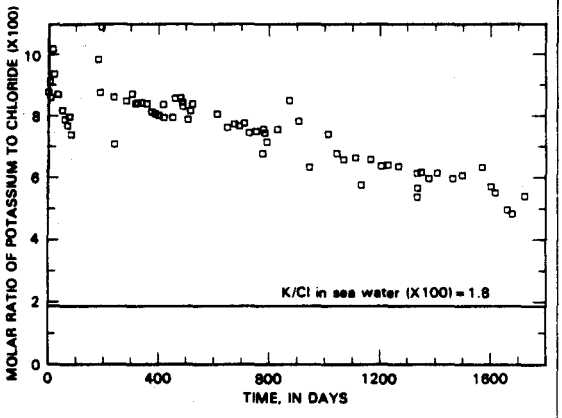

FIGURE 56.14.—Potassium-ion to chloride-ion ratio in HGP-A brines versus duration of production. Straight line represents potassium to chloride ratio in sea water.

of magnesium ion to the formation of magnesium oxysulfate ($MgO \cdot nMgSO_4 \cdot (n-2)H_2O$; Bischoff and Seyfried, 1978), a radical decline in pH, and an increase in the sea-water buffering capacity due to the presence of weak acids such as HCO_3^-, HSO_4^-, and HCl^0, and of $MgOH^+$, a weak base. These chemical changes occur progressively over a temperature of approximately 70–350 °C and are independent of sea water-basalt reactions. When sea water is heated in the presence of basalt, the increased hydrogen-ion concentration and buffering ability of the fluid drives numerous reactions that proceed only very slowly or not at all at lower temperatures and include the alteration of residual glass and primary calcic and sodic mineral suites to smectites, mixed layer clays, and chlorite. These reactions result in the removal of potassium and lithium from basalt, exchange of calcium for the magnesium lost from sea water, and under some conditions, depletion of sodium from sea water.

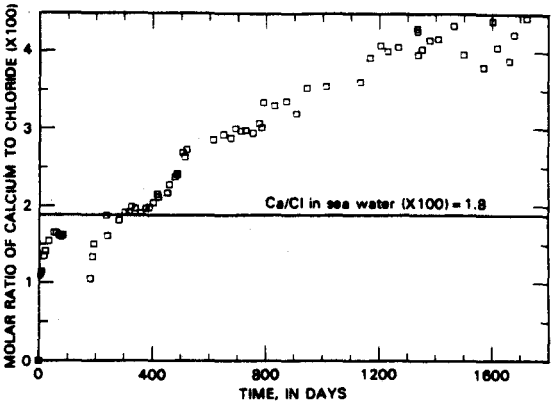

FIGURE 56.15.—Calcium-ion to chloride-ion ratio in HGP-A brines versus duration of continuous production. Straight line represents calcium to chloride-ion ratio in sea water.

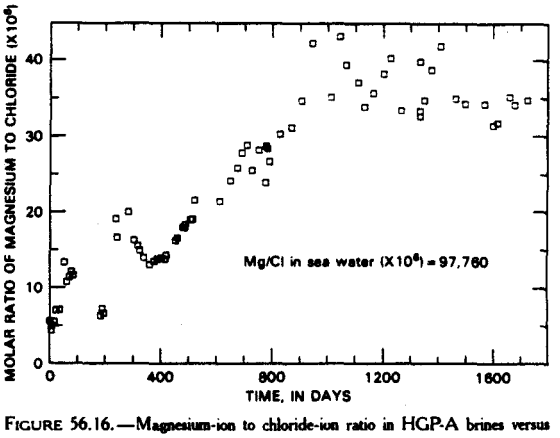

FIGURE 56.16.—Magnesium-ion to chloride-ion ratio in HGP-A brines versus duration of continuous production. Magnesium to chloride ratio in sea water is a factor of approximately 20,000 above that in HGP-A brine and is not plotted.

The hydrolysis of the primary silicates to the alteration-mineral assemblage buffers the pH of the sea water-basalt system at approximately 6.8 as long as primary minerals are available to exchange Ca for H^+ released by the loss of $Mg(OH)_2$. However, under sea water-dominated conditions, when the total magnesium available from sea water exceeds the potassium and calcium present in the basalt, pH will be buffered in the range of 2–3 depending upon temperature. This condition has been found to occur at sea water:rock ratios of approximately 50 and above (Mottl and Seyfried, 1980).

The alteration mineral suite typically generated by these reactions includes: zeolite, montmorillonite, illite, anhydrite, magnetite, pyrite, quartz, chlorite, epidote, actinolite (Mottl and Seyfried, 1980; Reed, 1982; Seyfried and Mottl, 1982). The conditions under which an individual mineral species is generated or is stable depends upon kinetics, temperature, and water:rock (W:R) ratios. Although a detailed discussion of the theoretical modeling of mineral stability (Helgeson and others, 1981; Reed, 1982, 1983; Reed and Spycher, 1984) is beyond the scope of the present discussion, the most pertinent findings of these studies to the present analysis are that: high temperatures and low W:R ratios favor epidote, actinolite, and pyrite deposition; high W:R ratios favor chlorite deposition; and cooling hydrothermal fluids precipitate pyrite and, at low W:R ratios, magnetite.

The current depletions of magnesium and sulfate and enrichments of lithium, potassium, and calcium in the fluids at HGP-A are consistent with the theoretical and experimental studies of the sea water-basalt system. The evolution of the chemical composition with time, from the initial production chemistry to the present, further indicates that the apparent W:R ratio has changed during the 4-yr discharge of HGP-A. Calculation of this ratio, using the potassium-ion enrichment of the sea-water component suggests that it was initially substantially less than 1 and that the present ratio approaches 2. A plot of the relative proportions of the three ions most sensitive to the W:R ratio further demonstrates its evolution with time (fig. 56.17). The trends evident in the changing ion ratios suggest an increasing calcium and magnesium concentration relative to potassium. Comparison of the trend in the brine chemistry with laboratory-derived data suggests that, as the sea water:rock ratios evolve, calcium ion will initially predominate at W:R ratios of approximately 10 and, as the ratio increases, magnesium will begin to displace calcium as the major component. More importantly, as the magnesium and W:R ratio increases, the pH will begin to decline due to the depletion of calcium from the reservoir rock (Mottl and Seyfried, 1980; Seyfried and Mottl, 1982). As the pH declines, the reservoir fluids will become far more aggressive and begin to mobilize higher concentrations of transition elements such as iron, lead, zinc, and tin.

A second aspect of the changing brine chemistry is the apparent change in reservoir temperatures that can be calculated. The reservoir temperatures calculated using the Na-K-Ca geothermometer initially indicated a temperature of approximately 300 °C; the silica geothermometer when corrected for steam loss (Fournier and Potter, 1982) yielded a temperature of 305 °C, in good agreement with the Na-K-Ca geothermometer. Na-K-Ca temperatures calculated using later chemical data from HGP-A have shown a decline in the calculated temperatures to approximately 250 °C (table 56.3). Silica, however, does not show a similar temperature change. The declining temperature calculated from the Na-K-Ca concentrations are interpreted to reflect the intrusion of lower temperature sea water into the intermediate-temperature aquifer tapped by HGP-A; the apparent discrepancy between the Na-K-Ca and silica temperatures is the result of the more rapid equilibration of silica to reservoir temperatures in the intruding fluids.

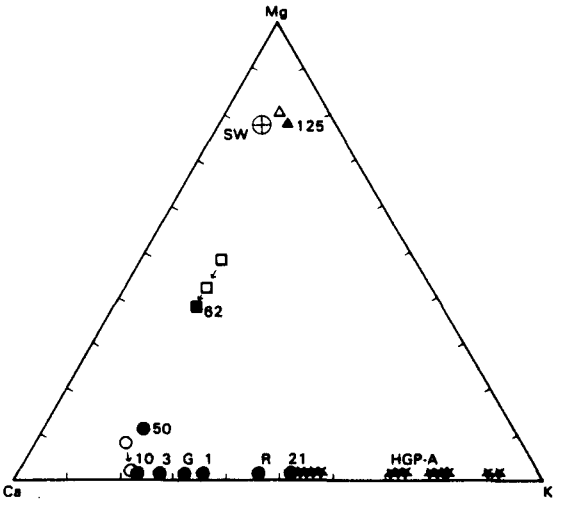

FIGURE 56.17.—Relative potassium-, calcium-, and magnesium-ion concentrations in: HGP-A geothermal brines (filled stars); hydrothermal vent fluids from 21° N., on East Pacific Rise (21) and Galapagos (G); Reykjanes geothermal system (R); liquid phase of high-temperature sea water-basalt experiments at water:rock ratios of 1, 3, 10, 50, 62, and 125 (labeled 1, 3, 10, 50, 62, and 125, respectively); and sea water (SW). Open symbols represent nonequilibrium compositions at noted water:rock ratios. HGP-A fluid chemistry has evolved from a relatively potassium-rich composition to an increasingly calcium-rich solution and is now approaching relative ion concentrations of fluids at 21° N.

The interpretation of the chemistry of the noncondensable gases in the HGP-A discharge is not as straightforward as that for the water chemistry, because two aquifers, having different gas concentrations, are supplying steam to the total flow in the well. Any attempt to partition the gases between the two production zones must rely on equilibrium calculations that will be dependent upon reservoir temperatures. A second aspect of the gas data that inhibits equilibrium calculations is that a significant proportion of the carbon dioxide present in the noncondensable gases is derived from surface sources and there is insufficient isotopic data to clearly differentiate the contributions from the available sources of carbon: sea water, ground water, and magmatic water.

In spite of these problems, several tentative interpretations of the gas chemistry can be offered. Comparison of the gas concentrations found in the steam at HGP-A with those found in laboratory sea water-basalt experiments tends to substantiate the W:R ratios inferred from the brine chemistry. Although mixing of the gas phase from the two production zones does not allow us to apportion the amount of gas from each, H_2S concentrations present in the total discharge (water plus steam) suggest that the average W:R ratio is well below 1 (Seyfried and Mottl, 1982). The decline in gas concentrations, although relatively minor, may further indicate that production of the reservoir is bringing about an increase in the effective W:R ratios. An alternative explanation of the decline in gas

concentrations may, however, be that the boiling front in the deeper reservoir has stabilized, yielding a constant steam:gas ratio.

Another noteworthy aspect of the gas produced by HGP-A is that a significant proportion of atmospheric carbon is present in the carbon dioxide: carbon-14 activities determined for the CO_2 have yielded apparent ages ranging from about 9–13 ka, or approximately 20 percent of modern carbon activities. Thus, at least 20 percent, or approximately 200 mg/kg of the 1,100 mg/kg of CO_2 in the steam phase is made up of surface carbon. This estimate is a minimum and presumes that the circulation rate in the rift is very short; a fluid residence time of 5,000 years would increase the proportion of atmospheric carbon to nearly 40 percent of the total. The source of this carbon is unclear; ground water typically contains CO_2 concentrations of only 10–20 ppm (U.S. Geological Survey, 1977) and, although sea water has a much higher concentration of CO_2, its relatively modest concentration in the reservoir fluids limits its contribution to approximately 20–30 mg/kg. The decline in CO_2 concentration during the period of increasing salinity has been accompanied by a slightly increased apparent age of the CO_2, and hence a sea-water source for the young carbon is not consistent with the observed trends in age and salinity. At present, no clear explanation is known for the carbon-14 data; it can only be stated that atmospheric carbon comprises a significant proportion of the CO_2 in the geothermal reservoir and that the fluid circulation time within the system is not more than 10,000 to 13,000 years.

The CO_2:H_2S ratio in the noncondensable gases in HGP-A is much lower than that found in most other geothermal systems where carbon dioxide predominates the noncondensable gases and is usually present at a concentration more than 2–5 times higher than H_2S. In the HGP-A fluids they are approximately equal when one considers the atmospheric contribution to the total CO_2. Two mechanisms can be proposed to account for the unusual CO_2:H_2S ratio found at HGP-A. The first is associated with the high-temperature reactions occurring in a sea water-basalt system: sea-water sulfate, at high temperature, oxidizes the reduced iron present in basalt to generate hematite and reduced sulfur by the reaction $8FeO + SO_4^{2-} \rightarrow 4Fe_2O_3 + S^{2-}$.

The high concentration of hematite identified in the intensely altered zones in HGP-A and other wells (Stone, 1977; Barnwell Geothermal Corp., unpublished data, 1985) are consistent with this model, but the relatively low concentration of sea water initially found in the HGP-A fluids suggests that this mechanism could supply only a modest amount of the sulfide found in the reservoir fluids.

The second mechanism that may account for the anomalous CO_2:H_2S ratio is that the magmas intruded into the ERZ may be depleted in magmatic carbon. Studies conducted by Gerlach and Graeber (1985) suggest that magma held in the summit magma chamber at Kilauea is preferentially degassed of the more-insoluble volatiles such as helium and carbon dioxide and that the magma later erupted from (and presumably intruded into) the ERZ shows a depletion of carbon relative to sulfur. Hence the low carbon to sulfur ratios observed in the geothermal fluids may be reflecting the C:S ratio present in the dike complex on the ERZ. Which of these mechanisms is ultimately responsible for the unusual C:S ratio in the HGP-A fluids cannot be determined at present; however, sulfur isotopic data currently being gathered may provide further insight into this question.

Although interpretation of the gas chemistry in terms of reservoir temperature is hindered by the mixing of the discharge from two production zones, a very crude estimate of the maximum and minimum temperatures indicated by the gas data can be obtained using the methane gas geothermometer of d'Amore and others (1982) and Nehring and d'Amore (1984) and making the assumptions that: (1) all of the gas present is associated with the deep steam-production zone; or (2) the well discharge is produced from a single aquifer. The gas compositions associated with these assumptions correspond to the gas concentration in the steam phase alone and that in the total discharge respectively and yield temperatures of 380 °C for the former and 350 °C for the latter. Both of these calculated temperatures are well above the Na-K-Ca and SiO_2 temperatures calculated for the brine phase, but are within the range of measured downhole temperatures in HGP-A and other nearby wells (358–368 °C). The modest change in the gas concentrations present in the HGP-A discharge do not yield an appreciable change in the gas geothermometry temperatures, indicating that production of steam from the deeper part of HGP-A has not been substantially affected by the intrusion of lower temperature fluids.

The few data available from the private exploration wells do not allow any definite conclusions to be drawn; however, the information available substantiates the interpretation of the HGP-A data. The salinity of the fluids in wells along the southern boundary of the rift tend to confirm the inferred structural control of the rift system over the fluid salinity in this hydrothermal system. The similarity of the gas concentrations present in the dry-steam wells and in HGP-A suggests that the majority of the noncondensable gas produced by HGP-A is coming from the deeper steam zone and, hence, the calculated gas geothermometer temperatures for the steam phase may more accurately reflect deep reservoir temperatures than does the calculation using the gas concentrations in the total discharge.

SYNTHESIS

The data that are presently available, although far from sufficient to allow a complete understanding of the hydrothermal system associated with the ERZ, provide at least preliminary constraints on a model of this unique geothermal reservoir. The physical dimensions of the hydrothermal system are defined by the location and age of intrusive bodies within the ERZ. The southern boundary apparently corresponds to the southernmost extent of recent eruptive features; temperature inversions in two wells drilled on this boundary demonstrate at least a localized temperature decline toward the south. The northern extent of the dike system is suggested by both geologic mapping and by geophysical models to be several kilometers north of the currently active part ofthe ERZ. However, due to heat loss with time, the temperatures present in the older parts of the ERZ probably will be much lower than those within the

currently active areas. Aeromagnetic data are in agreement with this model and suggest that temperatures in excess of the Curie point (560 °C) are present beneath the southern part of the ERZ but are lower to the north and south of the currently active rift.

The low salinities found in the deep reservoir fluids at HGP-A suggest that sea water is effectively excluded from the interior of the ERZ and that the overall hydrology within the reservoir is controlled by the rift-zone structure. Fluid flow within the ERZ is governed by the near-vertical tabular dikes comprising the rift and its associated fracture system, which trend in a northeast-southwest direction. The fractures effectively channel fresh meteoric water along the ERZ and to depth in the hydrothermal system, whereas the impermeable dike system and chemical self-sealing serve to inhibit intrusion of saline water from the south. Fresh water entering the ERZ in the upper elevations of the Kilauea flank penetrate to depth, are heated within the dike complex, and are discharged at the lower elevation eastern end of the subaerial part of the rift zone. The discharge of hydrothermal fluids in this region is confirmed by surface resistivity data, by ground-water temperature and chemistry data, and by the chemistry of the hydrothermal-alteration products found in the deep wells drilled into the LERZ.

The boundary between the meteorically derived hydrothermal fluids within the ERZ and saline fluids south of the ERZ is indicated to be quite sharp by the deep drilling data obtained on the LERZ: HGP-A had an initial chloride concentration of approximately 1,000 mg/kg and a bottom-hole temperature of 358 °C. The Lanipuna 1 sidetrack well, 2883-04A, located less than 500 m south of HGP-A, had an initial chloride content of about 19,000 mg/kg and a bottom-hole temperature of 149 °C.

The chemistry of the fluids circulating within the ERZ zone is strongly controlled by fracturing in the reservoir. Data from drill cuttings indicate that extreme alteration of basalt occurs intermittently down the geologic column and the alteration mineral suite is clearly generated from sea water-basalt reactions. Thus, access of sea water to the hydrothermal system does occur; laboratory and field studies of sea water-basalt reactions have demonstrated that W:R ratios can strongly influence both the salinity and the pH of the hydrothermal fluids, and therefore in those parts of the reservoir where sea water is present at high W:R ratios, the pH of the fluids may be much lower (and more aggressive) than those currently found in the interior of the ERZ.

CONCLUSION

A young, actively evolving hydrothermal system is associated with the Kilauea east rift zone. Its physical characteristics range from near-surface ambient conditions to temperatures and pressures approaching the critical point of water. Its chemistry varies from low-salinity, near-neutral fluids to strongly acid, highly aggressive saline fluids. Further study of this system will not only provide further insight into the geothermal conditions present in this reservoir, it may also add to the understanding of chemical cycling in other land-based and submarine hydrothermal systems.

REFERENCES

Bischoff, J.L., and Dickson, F.W., 1975, Seawater-basalt interaction at 200 °C and 500 bars: Implications for origin of seafloor heavy metal deposits and regulation of seawater chemistry: Earth and Planetary Science Letters, v. 25, p. 385-397.

Bischoff, J.L., and Seyfried, W.E., 1978, Hydrothermal chemistry of seawater from 25 ° to 350 °C: American Journal of Science, v. 278, no. 6, p. 838-860.

Cox, M.E., and Thomas, D.M., 1979, Cl/Mg ratio of Hawaiian groundwaters as a regional geothermal indicator in Hawaii: Hawaii Institute of Geophysics Technical Report, HIG-79-9, 51 p.

D'Amore, F., Celati, R., and Calore, C., 1982, Fluid geochemistry applications in reservoir engineering (vapor dominated systems): Stanford University, Proceedings of the Eighth Workshop on Geothermal Reservoir Engineering, Dec. 1982, p. 295-307.

Davis, D.A., and Yamanaga, G., 1968, Preliminary report on the water resources of the Hilo-Puna area, Hawaii: Circular C45, State of Hawaii, Honolulu, Division of Water and Land Development, Department of Land and Natural Resources, State of Hawaii, 124 p.

Druecker, M., and Fan, P.F., 1976, Hydrology and chemistry of groundwater in Puna, Hawaii: Ground Water, v. 14, no. 5, p. 328- 338.

Duffield, W.A., Christiansen, R.L., Koyanagi, R.Y., and Peterson, D.W., 1982, Storage, migration, and eruption of magma at Kilauea Volcano, Hawaii, 1971–1972: Journal of Volcanology and Geothermal Research, v. 13, p. 273-307.

Dzurisin, D., 1981, Changed magma budget since 1975 at Kilauea Volcano, Hawaii: Eos, Transactions, American Geophysical Union, v. 62, no. 45, p. 1071.

Fiske, R.S., and Jackson, E.D., 1972, Orientation and growth of Hawaiian volcanic rifts: the effect of regional structure and gravitational stresses: Proceedings of the Royal Society of London, Series A, v. 329, p. 299-326.

Fournier, R.O., 1981, Application of water geochemistry to geothermal exploration and reservoir engineering, *in* Ryback, L., and Muffler, L.J.P., eds., Geothermal systems, principals and case histories: p. 109-144.

Fournier, R.O., and Potter, R.W., II, 1982, A revised and expanded silica (quartz) geothermometer: Geothermal Resources Bulletin, v. 11, no. 10, p. 3-12.

Fournier, R.O., and Rowe, J.J., 1966, Estimation of underground temperatures from the silica content of water from hot springs and wet steam wells: American Journal of Science, v. 264, p. 685-697.

Fournier, R.O., and Truesdell, A.H., 1973, An empirical Na-K-Ca geothermometer for natural waters: Geochimica et Cosmochimica Acta, v. 37, no. 5, p. 1255-1275.

Furumoto, A.S., 1978, Nature of the magma conduit under the east rift zone of Kilauea Volcano, Hawaii: Bulletin Volcanologique, v. 41, no. 4, p. 435-453.

Gerlach, T., and Graeber, E.J., 1985, Volatile budget of Kilauea Volcano: Nature, v. 313, p. 273-277.

Godson, R.H., Zablockie, C.J., Pierce, H.A., Frayser, J.B., Mitchell, C.M., and Sneddon, R.A., 1981, Aeromagnetic map of the island of Hawaii: U.S. Geological Survey Geophysical Investigation Map GP-946, 1 sheet, scale 1:250,000.

Helgeson, H.C., Kirkham, D.H., and Flowers, G.C., 1981, Theoretical prediction of the thermodynamic behavior of aqueous electrolytes at high pressures and temperatures: IV. Calculation of activity coefficients, osmotic coefficients, and apparent molal and standard and relative partial molal properties to 600 °C and 5 kb: American Journal of Science, v. 281, no. 10, p. 1249-1516.

Holcomb, R.T., 1980, Preliminary geologic map of Kilauea Volcano, Hawaii: U.S. Geological Survey Open-File Report 80–796, 2 sheets, scale 1:50,000.

Humphris, S.E., and Thompson, G., 1978, Hydrothermal alteration of oceanic basalts by seawater: Geochimica et Cosmochimica Acta, v. 42, p. 107-125.

Iovanitti, J.L., and D'Olier, W.L., 1984, Preliminary results of drilling and testing in the Puna Geothermal System, Hawaii: Stanford University, Proceedings of the Tenth Workshop on Geothermal Reservoir Engineering, December 1984.

Kauahikaua, J.P., 1981, Interpretation of time-domain electromagnetic soundings in

the east-rift geothermal area of Kilauea Volcano, Hawaii: U.S. Geological Survey Open-File Report 81–979, 25 p.

Kauahikaua, J.P., Mattice, M.D., and Jackson, D.B., 1980, Mise-a-la-masse mapping of the HGP-A geothermal reservoir, Hawaii: Geothermal: Energy For the Eighties, Geothermal Research Council Transactions, v. 4, p. 65-68.

Kauahikaua, J.P., Zablockie, C.J., and Jackson, D.B., 1979, Controlled source electromagnetic mapping at the summit of Kilauea Volcano, Hawaii: Eos, Transactions, American Geophysical Union, v. 60, no. 46, p. 811-812.

Keller, G.V., Skokan, C.K., Skokan, J.J., Daniels, J., Kauahikaua, J.P., Klein, D.P., and Zablocki, C.J., 1977, Geoelectric studies on the east rift, Kilauea Volcano, Hawaii Island: Hawaii Institute of Geophysics Technical Report HIG 77-15.

Kristmannsdottir, H., 1976, Hydrothermal alteration of basaltic rocks in Icelandic Geothermal areas, *in* Proceedings of Second United Nations Symposium on the Development and Use of Geothermal Resources, San Francisco, Calif.: Washington, U.S. Government Printing Office, v. 1, p. 441-445.

Kroopnick, P.M., Lau, L.S., Buddemeier, R.W., Thomas, D.M., Lau, L.S., and Bills, D., 1978, Hydrology and geochemistry of a Hawaiian geothermal system: HGP-A. Hawaii Institute of Geophysics Technical Report HIG-78-6, 64 p.

Macdonald, G.A., Abbott, A.B., and Peterson, F., 1983, Volcanoes in the sea: The geology of Hawaii: Honolulu, University of Hawaii Press, 517 p.

Mink, J.F., 1977, Handbook—Index of Hawaii groundwater and resources data, v. I: Honolulu, University of Hawaii, Water Resources Research Center, Technical Report No. 113, 96 p.

Moore, R.B., 1983, Distribution of differentiated tholeiitic basalts on the lower east rift zone of Kilauea Volcano, Hawaii: A possible guide to geothermal exploration: Geology, v. 11, no. 3, p. 136-140.

Mottl, M.J., 1983, Metabasalts, axial hot springs, and the structure of hydrothermal systems at mid-ocean ridges: Geological Society of American Bulletin, v. 94, p. 161-180.

Mottl, M.J., and Holland, H.D., 1978, Chemical exchange during hydrothermal alteration of basalt by seawater—I: Experimental results for major and minor components of seawater: Geochimica et Cosmochimica Acta, v. 42, p. 1103-1115.

Mottl, M.J., and Seyfried, W.E., 1980, Subseafloor hydrothermal systems: rock-vs. seawater-dominated, *in* Rona, P.A., and Lowell, R.P., eds., Seafloor spreading centers: Hydrothermal Systems: Stroudsberg, Pa., Dowden, Hutchinson and Ross, Inc., 424 p.

Nehring, N.L., and D'Amore, F., 1984, Gas chemistry and thermometry of the Cerro Prieto, Mexico, geothermal field: Geothermics, v. 13, p. 75-89.

Pohl, D.C., and Liou, J.G., 1983, Flow-through reaction of basalt glass and seawater at 300° and 200 °C, 250 bars pressure [abs.]: Misasa, Japan, Fourth International Symposium on Water-Rock Interaction, Aug. 29–Sept. 3, 1983, p. 389-392.

Reed, M.H., 1982, Calculations of multicomponent chemical equilibria and reaction processes in systems involving minerals, gases, and an aqueous phase: Geochimica et Cosmochimica Acta, v. 46, p. 513-528.

——— 1983, Seawater-basalt reaction and the origin of greenstones and related ore deposits: Economic Geology, v. 78, p. 466-485.

Reed, M.H., and Spycher, N., 1983, Calculated pH at high temperature in hydrothermal waters with applications to geothermometry: Misasa, Japan, Fourth International Symposium on Water-Rock Interaction, Aug. 29–Sept. 3, 1983, p. 401-404.

——— 1984, Calculation of pH and mineral equilibria in hydrothermal waters with applicaton to geothermometry and studies of boiling and dilution: Geochimica et Cosmochimica Acta, v. 48, p. 1479-1492.

Seyfried, W.E., Jr., and Bischoff, J.L., 1981, Experimental seawater-basalt interaction at 300 °C, 500 bars, chemical exchange, secondary mineral formation and implications for the transport of heavy metals: Geochimica et Cosmochimica Acta, v. 45, p. 135-147.

Seyfried, W.E., and Mottl, M.J., 1982, Hydrothermal alteration of basalt by seawater under seawater-dominated conditions: Geochimica et Cosmochimica Acta, v. 46, p. 985-1002.

Shupe, J.W., Helsley, C.E., and Yuen, P.C., 1978, The Hawaii geothermal project: Summary report for phases I, II, and III: U.S. Department of Energy Report SAIV-1093-T6.

Stearns, H.T., and Macdonald, G.A., 1946, Geology and groundwater resources of the Island of Hawaii: Honolulu, Hawaii Division of Hydrography, Bulletin B9, 363 p.

Stone, C., 1977, Chemistry, petrography, and hydrothermal alteration of basalts from HGP-A, Kilauea, Honolulu, University of Hawaii, M.S. Thesis No. 1477, 84 p.

Stone, C., and Fan, P.F., 1978, Hydrothermal alteration of basalts from Hawaii Geothermal Project Well-A Kilauea, Hawaii: Geology, v. 6, p. 401-404.

Swanson, D.A., Duffield, W.A., and Fiske, R.S., 1976, Displacement of the south flank of Kilauea Volcano: The result of forceful intrusion of magma into the rift zones: U.S. Geological Survey Professional Paper 963, 39 p.

Takasaki, K.J., 1978, Summary appraisals of the nation's groundwater resources—Hawaii Region: U.S. Geological Survey Professional Paper 813–M, 175 p.

Thomas, D.M., 1980, Water and gas chemistry from the HGP-A geothermal well: January 1980 flow test: Geothermal Resources Council Transactions, v. 4, p. 181-184.

——— 1982, A geochemical case history of the HGP-A well 1976-1982, *in* Proceedings of the Pacific geothermal conference 1982 incorporating the 4th New Zealand geothermal workshop: Auckland, N.Z., University of Auckland Geothermal Institute, p. 273-278.

Thomas, D.M., and Sakai, H., 1983, Chemical and isotopic studies of the HGP-A geothermal well [abs.]: Misasa, Japan, Fourth International Symposium on Water-Rock Interaction, Aug. 29–Sept. 3, 1983, p. 479-482.

Tomasson, J., and Kristmannsdottir, H., 1972, High temperature alteration minerals and thermal brines, Reykjanes, Iceland: Contribution to Mineralogy and Petrology, v. 36, p. 123-134.

U.S. Geological Survey, 1977, Water resources data for Hawaii and other Pacific areas: Water year 1977, v. 10: U.S. Geological Survey Water-Data Report HI-77-1, 348 p.

Waibel, A., 1983, A review of the hydrothermal mineralogy of Hawaii Geothermal Project Well-A, Kilauea, Hawaii: Geothermal Resources Council Transactions, v. 7, p. 205-209.

Yuen, P.C., Chen, B.H., Kihara, D.H., Seki, A.S., and Takahashi, P.K., 1978, The Hawaii geothermal project: HGP-A and reservoir engineering: Honolulu, University of Hawaii, Hawaii Geothermal Project internal report, 96 p.

Zablocki, C.J., 1976, Mapping thermal anomalies on an active volcano by the self-potential method, Kilauea, Hawaii: Second U.N. Symposium on the Development and Use of Geothermal Resources, Proceedings, v. 2, p. 1299-1309.

———1977, Self-potential studies in east Puna, Hawaii, *in* Geoelectric studies on the east rift, Kilauea Volcano, Hawaii Island: Hawaii Institute of Geophysics Technical Report HIG-77-15, p. 175-195.